Active DNA demethylation in plant companion cells reinforces transposon methylation in gametes

Christian A. Ibarra[1*], Xiaoqi Feng[1*], Vera K. Schoft[2*], Tzung-Fu Hsieh[1*], Rie Uzawa[1], Jessica A. Rodrigues[1], Assaf Zemach[1], Nina Chumak[2], Adriana Machlicova[2], Toshiro Nishimura[1], Denisse Rojas[1], Robert L. Fischer[1†], Hisashi Tamaru[2†], Daniel Zilberman[1†]

[1]Department of Plant and Microbial Biology, University of California, Berkeley, CA, USA.

[2]Gregor Mendel Institute, Austrian Academy of Sciences, Vienna, Austria.

[*]These authors contributed equally.

[†]To whom correspondence should be addressed. E-mail: rfischer@berkeley.edu, hisashi.tamaru@gmi.oeaw.ac.at, danielz@berkeley.edu.

Summary

Active DNA demethylation in the companion cells of plant gametes mediates methylation of gamete transposons.

Abstract

The *Arabidopsis thaliana* central cell, the companion cell of the egg, undergoes DNA demethylation prior to fertilization, but the targeting preferences, mechanism, and biological significance of this process remain unclear. Here, we show that active DNA demethylation mediated by the DEMETER DNA glycosylase accounts for all of the demethylation in the central cell, and preferentially targets small, AT-rich and nucleosome-depleted euchromatic transposable elements. The vegetative cell, the companion cell of sperm, also undergoes DEMETER-dependent demethylation of similar sequences, and lack of DEMETER in vegetative cells causes reduced small RNA-directed DNA methylation of transposons in sperm. Our results demonstrate that demethylation in companion cells reinforces transposon methylation in plant gametes and likely contributes to stable silencing of transposable elements across generations.

Cytosine methylation regulates gene expression and represses transposable elements (TEs) in plants and vertebrates (*1*). DNA methylation in plants is catalyzed by three families of DNA methyltransferases that can be roughly grouped by the preferred sequence context: CG, CHG, and CHH (H = A, C or T). The small RNA (sRNA) pathway targets *de novo* methylation in all sequence contexts, and is required for the maintenance of CHH methylation.

Flowering plant sexual reproduction involves two fertilization events (*2*). The pollen vegetative cell forms a tube that carries two sperm cells to the ovule, where one fuses with the diploid central cell to form the triploid placenta-like endosperm, and the other fertilizes the haploid egg to produce the embryo. Endosperm DNA of *Arabidopsis thaliana* is modestly but globally less methylated than embryo DNA in all contexts (*3*). The DEMETER (DME) DNA glycosylase that excises 5-methylcytosine is highly expressed in the central cell prior to fertilization and is at least partially required for the demethylation observed in endosperm (*2, 3*), which has been inferred to occur on the maternal chromosomes inherited from the central cell. Passive mechanisms, such as downregulation of the MET1 DNA methyltransferase, have also been proposed to contribute to demethylation of the maternal endosperm genome (*2*). The global differences between embryo and endosperm are consistent with passive demethylation, and suggest that the process may have little sequence specificity (*3, 4*). However, DNA methylation has not been compared between the maternal and paternal endosperm genomes except for a few loci, and therefore it is difficult to make general inferences about the mechanism and specificity of central cell demethylation. Why the central cell should undergo extensive DNA demethylation is also unclear.

To understand the extent, mechanism and biological significance of active demethylation in the central cell, we used reciprocal crosses between the Col and L*er* accessions of *Arabidopsis* that differ by over 400,000 single nucleotide polymorphisms (SNPs) (*4*) to identify DNA methylation that resides on either the maternal or paternal endosperm genome (*5*) by shotgun bisulfite sequencing (table S1). The wild-type maternal genome is substantially less methylated than the paternal genome in the CG context (Fig. 1A and S1-2), with slight global hypomethylation accompanied by strong local demethylation (Fig. 1B and S3-4). The local demethylation is nearly fully reversed in *dme* mutant endosperm (Fig. 1A-B, S2, S4-5), indicating that DME is either the only or by far the major enzyme required for excision of 5-methylcytosine in the central cell, and demonstrating that active DNA demethylation of at least 9,816 specific sequences spanning 4,443,250 bp (table S2) accounts for the methylation differences between the maternal and paternal endosperm genomes. Global CG methylation of both maternal and paternal genomes is slightly elevated by lack of DME compared to wild-type (Fig. 1A and S5), consistent with overexpression of genes that mediate CG methylation in *dme* endosperm (*4*).

Global CHG methylation of the wild-type endosperm maternal genome is similar to that of the paternal genome (Fig. 1C-D), but loci that are maternally demethylated in the CG context show strong maternal CHG demethylation (Fig. 1D), consistent with the reported *in vitro* activity of DME on methylation in all sequence contexts (*6*). A similar but weaker correspondence exists for CHH methylation (Fig. 1E-F), presumably because sRNA-directed DNA methylation (RdDM) patterns are more variable, and may be partially restored after fertilization. We did not observe major methylation differences between parental genomes in embryo (Fig. 1A, C, E, S1-2, S4 and S6).

As we showed previously, *dme* endosperm has greatly reduced CHG methylation and almost no CHH methylation (*3*), and our present data show that this applies similarly to both parental genomes (Fig. 1C, E and S2). As this is the opposite of the outcome expected from a mutation in a demethylating enzyme, we hypothesized an indirect mechanism. DME activity is required for functionality of the Polycomb Repressive Complex 2 (PRC2) in endosperm, prompting us to examine methylation in endosperm lacking maternal activity of the core PRC2 protein FIE (*2*). Lack of FIE had an effect similar to that of lack of DME on non-CG methylation (Fig. 1C, E and table S1), demonstrating that PRC2 promotes non-CG DNA methylation in endosperm. In contrast, local maternal CG demethylation was mostly unaffected by lack of FIE (Fig. 1B, and S4-5), as would be expected with direct activity of DME. Global CG methylation levels were increased even more than in *dme* endosperm (Fig. 1A and S5), consistent with strong overexpression of genes that mediate CG methylation in *fie* endosperm (*4*).

DME-mediated DNA demethylation in the central cell is required to establish monoallelic (imprinted) expression of a number of genes in the endosperm (*2, 4*). We examined the location of loci that are significantly less methylated in wild-type endosperm than in *dme* endosperm (table S2) in relation to imprinted endosperm genes (fig. S4). Maternally and paternally expressed genes are preferentially associated with such differentially methylated regions (DMRs), particularly just upstream of the gene (fig. S7). Maternally expressed genes also exhibit DMRs that span the transcriptional start site (fig. S7), consistent with the strong correlation between methylation of this region and gene silencing (*1*). Paternally expressed genes are enriched in DMRs within the gene body (fig. S7), suggesting that gene body demethylation can disrupt gene expression, for example by revealing repressor binding sites, as has been proposed for the DMR downstream of the *PHERES1* gene (fig. S4) (*2*).

Several TEs were reported to be less methylated in the pollen vegetative cell of *Arabidopsis* compared to sperm (*7*), and we recently showed that DME is required for demethylation of two genes in the vegetative cell that are demethylated by DME in the central cell (*8*). These data suggest that DME-mediated DNA demethylation may proceed similarly in the central and vegetative cells. To examine this issue, we compared DNA methylation patterns in sperm and vegetative cell nuclei that were purified by fluorescence activated cell sorting (*8, 9*). Most CG sites are heavily and similarly methylated in both cell types, but a subset is specifically demethylated in the vegetative cell (Fig. 2A-B, S3-4, S8), corresponding to at least 9,932 loci spanning 4,068,000 bp (table S2). The demethylated vegetative cell CG sites overlap 45.5% of those demethylated in the maternal endosperm genome, and by extension in the central cell (Fig. 2B, S4 and table S2).

We examined methylation in pollen from heterozygous *dme/+* plants (strong *dme* alleles cannot be made homozygous), in which half of the pollen lacks DME (*8*). CG sites that are demethylated in wild-type vegetative cells showed much greater methylation in vegetative cell nuclei isolated from *dme/+* pollen (Fig. 2A-B, and S4), indicating that DME is required for demethylation in the vegetative cell. CHG methylation is generally higher in the vegetative cell than in the sperm cell (Fig. 2C-D), but loci demethylated at CG sites in the vegetative cell are also demethylated at CHG sites (Fig. 2D), as they are in endosperm (Fig. 1D). CHH methylation is very high in the vegetative cell and low in sperm (Fig. 2E), consistent with the strong RdDM activity reported in the vegetative cell (*9*). Nonetheless, vegetative cell CG-demethylated loci tend to show lower CHH methylation in vegetative cells than in sperm (Fig. 2F). Overall, our data strongly support the hypothesis that DNA demethylation in the male and female companion cells proceeds by an active, DME-dependent mechanism.

Loci demethylated in companion cells tend to be within smaller AT-rich TEs that are enriched for euchromatin-associated histone modifications (*10*) and depleted of nucleosomes with heterochromatin-associated modifications (Fig. 3A-B and S9-10), suggesting that chromatin structure plays an important role in regulating active DNA demethylation (*11*), consistent with the decondensation of heterochromatin observed in central and vegetative cells (*9, 12*). TEs longer than 3 kb are rarely demethylated (Fig. 3A and S3), except at the edges (fig. S9), consistent with our published observations in rice (*13*). The preference for smaller TE demethylation holds for TEs of various types (fig. S10). Demethylation of small TEs accounts for the shapes of the wild-type maternal endosperm methylation traces (Fig. 1A, C, E) and the wild-type vegetative cell methylation traces (Fig. 2A, C), which are closer to the paternal and sperm traces, respectively, in the middle (long TEs) than at the points of alignment (mostly small TEs). Small *Arabidopsis* TEs, like their rice counterparts (*13*), tend to occur near genes (Fig. 3C), explaining the observation that DME and related glycosylases preferentially demethylate gene-adjacent sequences (Fig. 3C) (*2, 14, 15*). This phenomenon explains why CHG and CHH methylation is lower in wild-type vegetative cells compared to sperm near genes (fig. S8), even though overall non-CG methylation is higher in vegetative cells than in sperm (Fig. 2C-F).

The abundance of DME targets in gene-poor heterochromatin (fig. S11) and the overlap among DME targets in the central and vegetative cells (table S2), despite their different functions and developmental fates, suggest that establishment of genomic imprinting is not the basal function of DME. DNA demethylation and activation of TEs in the vegetative cell was proposed to generate sRNAs that would reinforce silencing of complementary TEs in sperm (*7*). If such TEs are demethylated in the central cell, their maternal copies should remain active in endosperm. Indeed, we identified 11 TEs demethylated by DME that are specifically maternally

expressed in wild-type, but not *dme* endosperm (Fig. 4A and table S4) (*4*). We also tested whether sRNAs can travel from the central cell to the egg by expressing a microRNA in the central cell that targets cleavage of GFP RNA expressed from a transgene in the egg, analogous to an experiment performed earlier in pollen (*7*). The central cell-expressed microRNA substantially reduced GFP fluorescence in the egg (fig. S12 and table S5), suggesting that central cell sRNAs can travel into and function in the egg.

If silencing induced by companion cell sRNAs occurs at the transcriptional level, lack of DME in the companion cell would be expected to reduce RdDM of DME target sequences in gametes. Indeed, overall CHH methylation of TEs is decreased in *dme/+* sperm compared to wild-type sperm (Fig. 2E), and CG sites demethylated by DME in vegetative cells show preferential CHH hypomethylation in *dme/+* sperm (Fig. 4B, D). Conversely, loci that exhibit decreased CHH methylation in *dme/+* sperm show increased CG methylation in *dme/+* vegetative cells (Fig. 4C-D). Thus, DME activity in the vegetative cell is required for full methylation of a subset of sperm TEs, indicating that demethylation in companion cells generates a mobile signal – probably sRNA – that immunizes the gametes against TE activation. This conclusion is supported by the specific CHH hypermethylation of small, endosperm-demethylated TEs observed in the rice embryo (*13*).

References

1. J. A. Law, S. E. Jacobsen, *Nature Reviews Genetics* **11**, 204 (2010).
2. M. J. Bauer, R. L. Fischer, *Curr Opin Plant Biol* **14**, 162 (2011).
3. T.-F. Hsieh *et al.*, *Science* **324**, 1451 (2009).
4. T.-F. Hsieh *et al.*, *Proc Natl Acad Sci U S A* **108**, 1755 (2011).
5. Materials and methods are available as supporting material on *Science Online*.
6. M. Gehring *et al.*, *Cell* **124**, 495 (2006).
7. R. K. Slotkin *et al.*, *Cell* **136**, 461 (2009).
8. V. K. Schoft *et al.*, *Proc Natl Acad Sci U S A* **108**, 8042 (2011).
9. V. K. Schoft *et al.*, *EMBO Rep* **10**, 1015 (2009).
10. F. Roudier *et al.*, *EMBO J* **30**, 1928 (2011).
11. W. Qian *et al.*, *Science* **336**, 1445 (2012).
12. M. Pillot *et al.*, *Plant Cell* **22**, 307 (2010).
13. A. Zemach *et al.*, *Proc Natl Acad Sci U S A* **107**, 18729 (2010).
14. R. Lister *et al.*, *Cell* **133**, 523 (2008).
15. J. Penterman *et al.*, *Proc Natl Acad Sci U S A* **104**, 6752 (2007).
16. See Supplementary Materials for acknowledgements. Sequencing data are deposited in GEO (GSE38935).

Fig. 1. Local DME-dependent demethylation of maternal endosperm chromosomes. (**A, C, E**) Transposons were aligned at the 5' and 3' ends (dashed lines) and average methylation levels for each 100-bp interval are plotted. (**B, D, F**) Kernel density plots trace the frequency distribution of endosperm methylation differences for all 50-bp windows with an informative SNP. A shift of the peak with respect to zero represents a global difference; shoulders represent local differences.

Fig. 2. Local DME-dependent demethylation in the pollen vegetative cell. (**A, C, E**) Average methylation in transposons was plotted as in Fig. 1. (**B, D, F**) Kernel density plots, as in Fig. 1, of pollen methylation differences in 50-bp windows.

Fig. 3. DME demethylates small, AT-rich euchromatic TEs. (**A**) Box plots showing absolute fractional demethylation of 50-bp windows within transposons. Each box encloses the middle 50% of the distribution, with the horizontal line marking the median, and vertical lines marking the minimum and maximum values that fall within 1.5 times the height of the box. Differences between each size category are significant ($p<0.001$, Kolmogorov-Smirnov test). (**B**) Significant ($p<0.001$, Kolmogorov-Smirnov test) Spearman correlation coefficients between extent of demethylation and chromatin features. (**C**) Distribution of transposable elements and significantly differentially methylated cytosines (DMCs; CG context; p-value < 0.0001, Fisher's exact test) with respect to genes.

Fig. 4. Demethylation activates TEs in companion cells and reinforces methylation in sperm. (**A**) DME-dependent demethylation of TEs that are maternally expressed in wild-type, but not *dme* endosperm (table S4). DMRs (table S2) are underlined. (**B**) Kernel density plots of the CHH methylation differences between sperm cells from wild-type and *dme*/+ plants. (**C**) Kernel density plots of the CG methylation differences between vegetative cells from wild-type and *dme*/+ plants. (**D**) Snapshots of CG and CHH methylation in pollen on chromosome 1. Arrows point out loci with decreased CHH methylation in sperm and increased CG methylation in vegetative cells from *dme*/+ pollen.

Figure 1

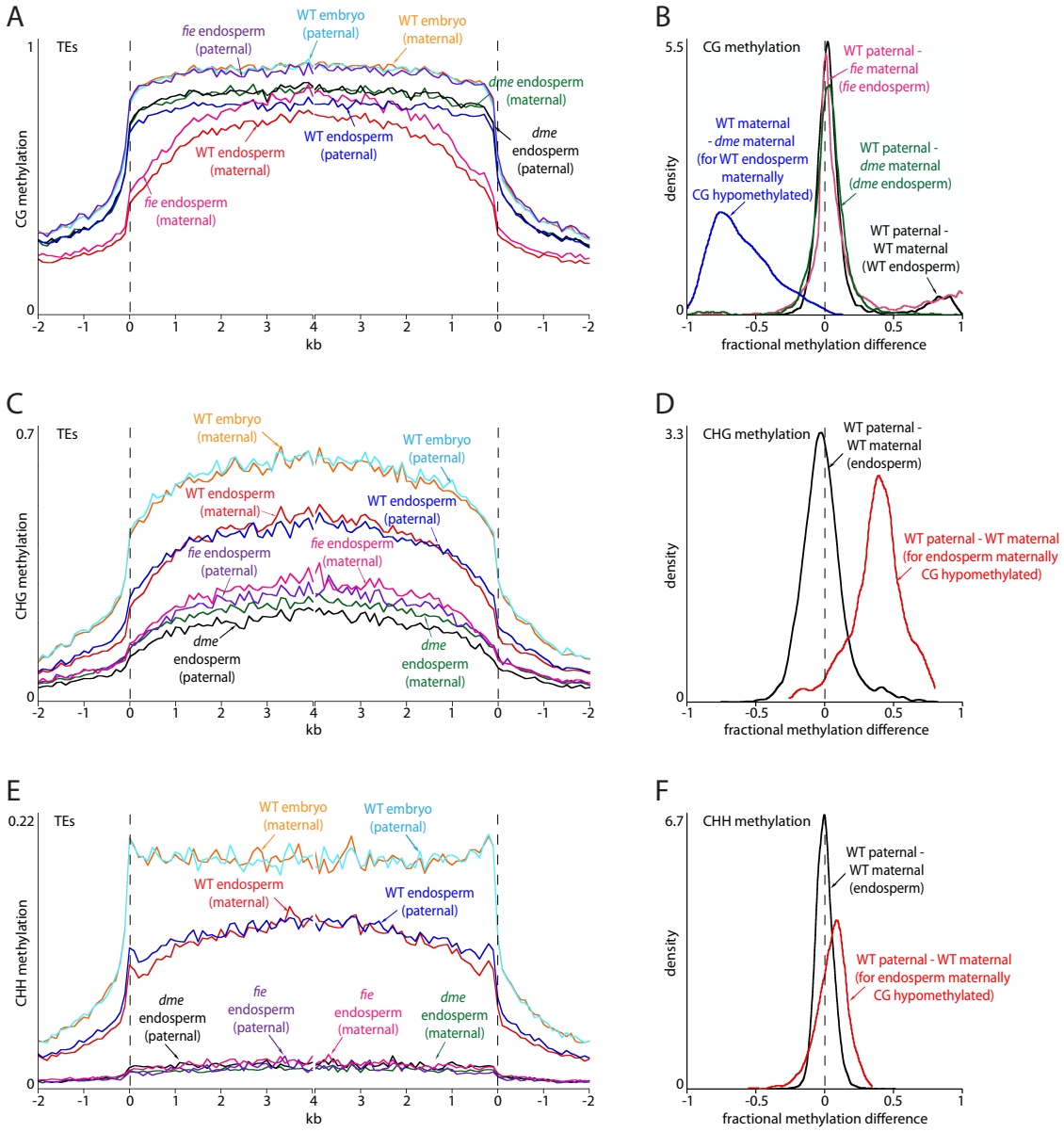
A
TEs
CG methylation
kb
WT embryo (paternal)
WT embryo (maternal)
fie endosperm (paternal)
dme endosperm (maternal)
dme endosperm (paternal)
WT endosperm (paternal)
WT endosperm (maternal)
fie endosperm (maternal)
B
CG methylation
density
fractional methylation difference
WT paternal - fie maternal (fie endosperm)
WT maternal - dme maternal (for WT endosperm maternally CG hypomethylated)
WT paternal - dme maternal (dme endosperm)
WT paternal - WT maternal (WT endosperm)
C
TEs
CHG methylation
kb
WT embryo (maternal)
WT embryo (paternal)
WT endosperm (maternal)
WT endosperm (paternal)
fie endosperm (paternal)
fie endosperm (maternal)
dme endosperm (paternal)
dme endosperm (maternal)
D
CHG methylation
density
fractional methylation difference
WT paternal - WT maternal (endosperm)
WT paternal - WT maternal (for endosperm maternally CG hypomethylated)
E
TEs
CHH methylation
kb
WT embryo (maternal)
WT embryo (paternal)
WT endosperm (maternal)
WT endosperm (paternal)
dme endosperm (paternal)
fie endosperm (paternal)
fie endosperm (maternal)
dme endosperm (maternal)
F
CHH methylation
density
fractional methylation difference
WT paternal - WT maternal (endosperm)
WT paternal - WT maternal (for endosperm maternally CG hypomethylated)

Figure 2

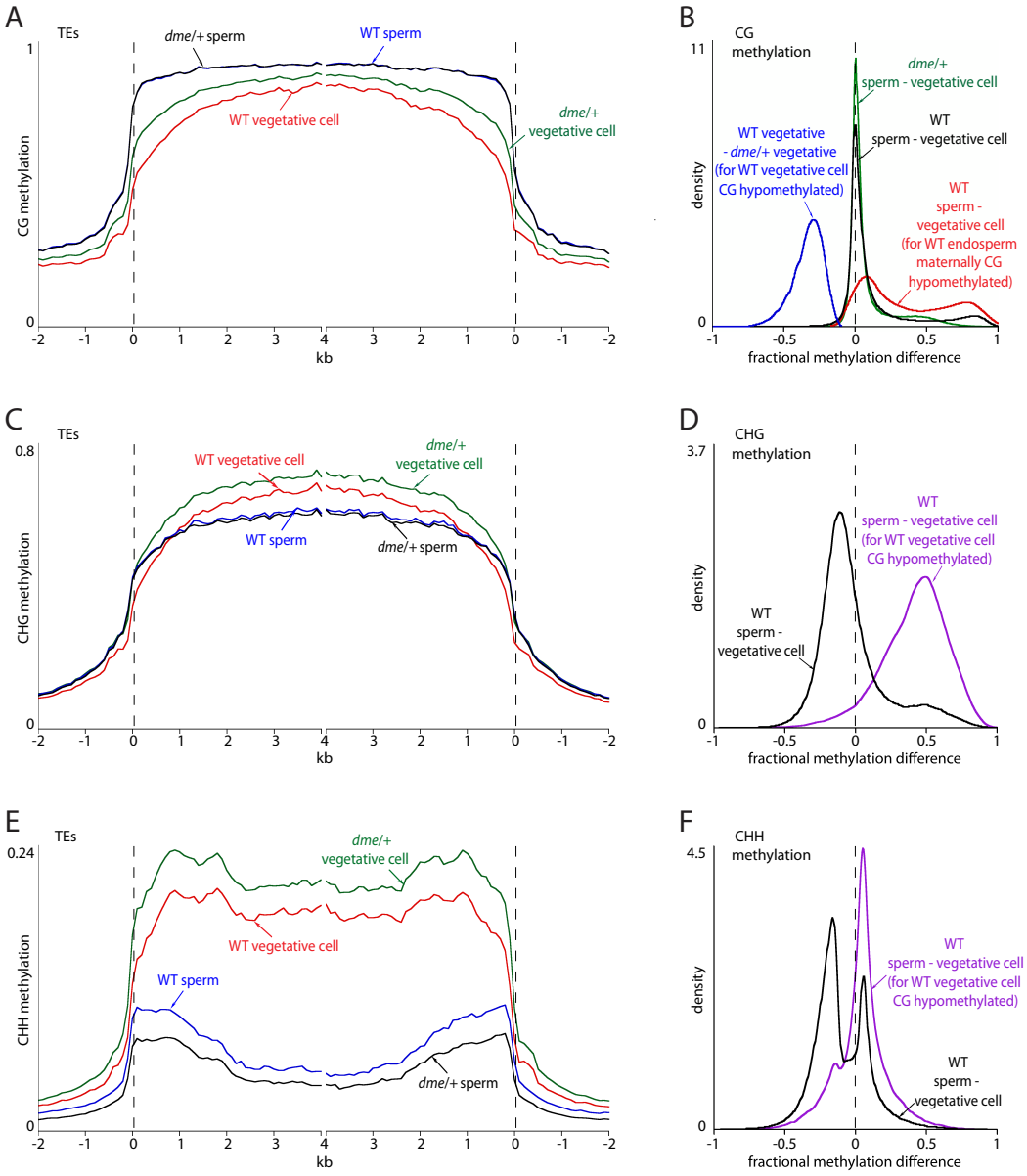
A
TEs
dme/+ sperm
WT sperm
WT vegetative cell
dme/+ vegetative cell
CG methylation
1
0
-2 -1 0 1 2 3 4 3 2 1 0 -1 -2
kb
B
CG methylation
11
dme/+ sperm - vegetative cell
WT sperm - vegetative cell
WT vegetative - dme/+ vegetative (for WT vegetative cell CG hypomethylated)
WT sperm - vegetative cell (for WT endosperm maternally CG hypomethylated)
density
0
-1 -0.5 0 0.5 1
fractional methylation difference
C
TEs
0.8
WT vegetative cell
dme/+ vegetative cell
WT sperm
dme/+ sperm
CHG methylation
0
-2 -1 0 1 2 3 4 3 2 1 0 -1 -2
kb
D
CHG methylation
3.7
WT sperm - vegetative cell (for WT vegetative cell CG hypomethylated)
WT sperm - vegetative cell
density
0
-1 -0.5 0 0.5 1
fractional methylation difference
E
TEs
0.24
dme/+ vegetative cell
WT vegetative cell
WT sperm
dme/+ sperm
CHH methylation
0
-2 -1 0 1 2 3 4 3 2 1 0 -1 -2
kb
F
CHH methylation
4.5
WT sperm - vegetative cell (for WT vegetative cell CG hypomethylated)
WT sperm - vegetative cell
density
0
-1 -0.5 0 0.5 1
fractional methylation difference

Figure 3

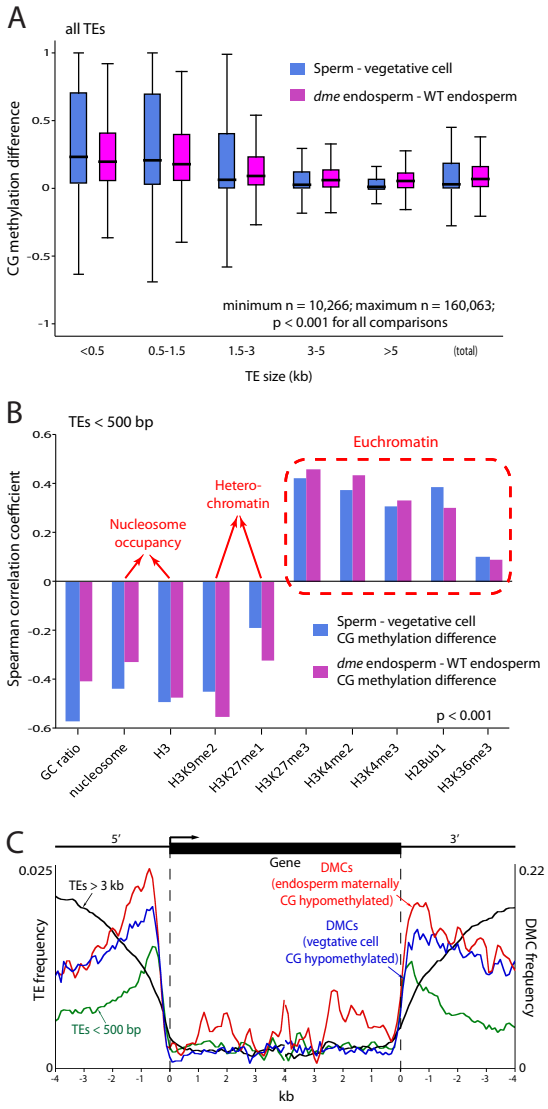
A
all TEs
Sperm - vegetative cell
dme endosperm - WT endosperm
CG methylation difference
minimum n = 10,266; maximum n = 160,063;
p < 0.001 for all comparisons
<0.5
0.5-1.5
1.5-3
3-5
>5
(total)
TE size (kb)
B
TEs < 500 bp
Euchromatin
Hetero-
chromatin
Nucleosome
occupancy
Spearman correlation coefficient
Sperm - vegetative cell
CG methylation difference
dme endosperm - WT endosperm
CG methylation difference
p < 0.001
GC ratio
nucleosome
H3
H3K9me2
H3K27me1
H3K27me3
H3K4me2
H3K4me3
H2Bub1
H3K36me3
C
5′
3′
Gene
DMCs
(endosperm maternally
CG hypomethylated)
DMCs
(vegtative cell
CG hypomethylated)
TEs > 3 kb
TEs < 500 bp
TE frequency
DMC frequency
kb

Figure 4

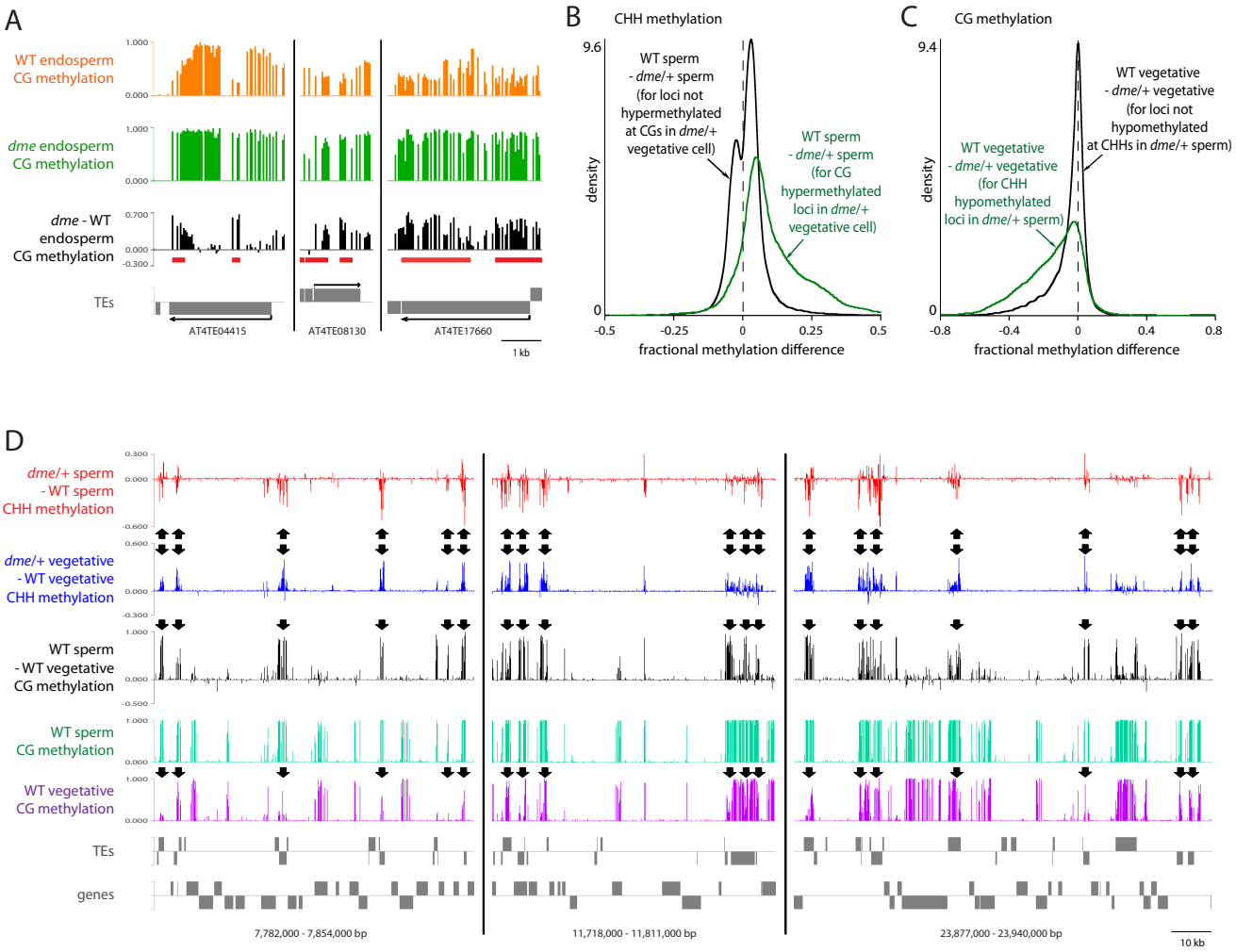
A
WT endosperm CG methylation
dme endosperm CG methylation
dme - WT endosperm CG methylation
TEs
AT4TE04415
AT4TE08130
AT4TE17660
1 kb
B
CHH methylation
WT sperm - dme/+ sperm (for loci not hypermethylated at CGs in dme/+ vegetative cell)
WT sperm - dme/+ sperm (for CG hypermethylated loci in dme/+ vegetative cell)
density
fractional methylation difference
C
CG methylation
WT vegetative - dme/+ vegetative (for loci not hypomethylated at CHHs in dme/+ sperm)
WT vegetative - dme/+ vegetative (for CHH hypomethylated loci in dme/+ sperm)
density
fractional methylation difference
D
dme/+ sperm - WT sperm CHH methylation
dme/+ vegetative - WT vegetative CHH methylation
WT sperm - WT vegetative CG methylation
WT sperm CG methylation
WT vegetative CG methylation
TEs
genes
7,782,000 - 7,854,000 bp
11,718,000 - 11,811,000 bp
23,877,000 - 23,940,000 bp
10 kb

Supplementary Materials for

Active DNA Demethylation in Plant Companion Cells Reinforces Transposon Methylation in Gametes

Christian A. Ibarra, Xiaoqi Feng, Vera K. Schoft, Tzung-Fu Hsieh, Rie Uzawa, Jessica A. Rodrigues, Assaf Zemach, Nina Chumak, Adriana Machlicova, Toshiro Nishimura, Denisse Rojas, Robert L. Fischer, Hisashi Tamaru, Daniel Zilberman.

correspondence to: rfischer@berkeley.edu, hisashi.tamaru@gmi.oeaw.ac.at, danielz@berkeley.edu.

This PDF file includes:

Materials and methods

Isolation of *A. thaliana* endosperm. Stage 12-13 flower buds were emasculated and pollinated 48 hours later. Reciprocal crosses were performed using wild-type Col-0 and L*er* ecotypes. In addition, *dme-2* (Col-*gl*) (*16*) heterozygous flowers were pollinated with wild-type (L*er*) pollen, and *fie-1* (L*er*) (*17*) heterozygous flowers were pollinated with wild-type (Col-0) pollen. For wild-type crosses, seven to eight days after pollination, F1 seeds (torpedo-stage to early-bent-cotyledon stage) were immersed in 0.3 M sorbitol and 5 mM Mes (pH 5.7) on a slide under a dissecting microscope. Embryo and endosperm were dissected using a fine needle and forceps. The seed coat was discarded. Wild-type embryos were twice centrifuged and the pellet resuspended in 0.3 M sorbitol and 5 mM Mes (pH 5.7) to remove contaminating endosperm. For crosses with the *dme-2* or *fie-1* mutations, F1 aborting seeds were identified and mutant endosperm was isolated. Approximately 500 wild-type endosperm, 1000 *dme-2* or *fie-1* endosperm, and 300 wild-type embryos were collected.

Isolation of vegetative cell and sperm nuclei. Pollen was isolated from wild-type (Col-0) and *dme-2* heterozygous plants (Col-*gl* ecotype) as described previously (*8, 9*). Vegetative cell and sperm nuclei were extracted from mature pollen and fractionated by fluorescence activated cell sorting as described previously (*8, 9*).

Bisulfite sequencing library construction. As described previously, genomic DNA was isolated from vegetative cell and sperm nuclei (*8*), endosperm, and embryo (*3*). Paired-end bisulfite sequencing libraries for Illumina sequencing were constructed as described previously (*3*) with minor modifications. In brief, about 150 ng of genomic DNA was fragmented by sonication, end repaired and ligated to custom-synthesized methylated adapters (Eurofins MWG Operon) according to the manufacturer's (Illumina) instructions for gDNA library construction. Adaptor-ligated libraries were subjected to two successive treatments of sodium bisulfite conversion using the EpiTect Bisulfite kit (Qiagen) as outlined in the manufacturer's instructions. One quarter of the bisulfite-converted libraries was PCR amplified using the following conditions: 2.5 U of ExTaq DNA polymerase (Takara Bio), 5 µl of 10X Extaq reaction buffer, 25 µM dNTPs, 1 µl Primer 1.1, 1 µl Primer 2.1 (50 µl final). PCR reactions were carried out as follows: 95℃ 3 min, then 12-14 cycles of 95℃ 30 sec, 65℃ 30 sec and 72℃ 60 sec. The enriched libraries were purified twice with solid phase reversible immobilization (SPRI) method using AM-Pure beads (Beckman Coulter) prior to quantification with a Bioanalyzer (Agilent). Sequencing on the Illumina platform was performed at the Vincent J. Coates Genomic Sequencing Laboratory at UC Berkeley and the Genome Center at UC Davis.

Allele-specific determination of DNA methylation. Reads were sorted to the Col and L*er* genomes as described (*4*). DNA methylation of cytosines within sorted reads was calculated as described (*3, 18*).

Gene and TE meta analysis (ends analysis). *A. thaliana* TAIR-annotated genes or transposons were aligned at the 5' end or the 3' end. For genes and TEs, we discarded from the analysis 1500 bp or 250 bp, respectively, from the end opposite to the one used for alignment to avoid averaging the edges of shorter genes and TEs with the middles of longer sequences.

Density plots. All DNA methylation kernel density plots compare fractional methylation within 50-bp windows. We used windows with at least 20 informative sequenced cytosines (10 for

CHG in endosperm) and fractional methylation of at least 0.7 (CG), 0.4 (CHG endosperm), 0.5 (CHG pollen), 0.08 (CHH endosperm), 0.15 (CHH vegetative cell), or 0.05 (CHH sperm) in at least one of the samples being compared. For parent-of-origin endosperm plots, only windows with methylation differences between Col and L*er* below 0.1 (CG), 0.15 (CHG), or 0.05 (CHH) were used to exclude ecotype-specific differences. Windows in which fractional paternal (or sperm) CG methylation exceeded fractional maternal (or vegetative cell) CG methylation by at least 0.4 were considered demethylated.

Box plots. Box plots compare fractional methylation in TEs within 50-bp windows and use the same cutoffs as density plots. To examine the correlation between CG demethylation and chromatin structure, TE windows are separated into five groups in ascending order according to GC ratio, nucleosome enrichment, dimethylation of lysine 9 of histone H3 (H3K9me2), and distance from the closest edge of the TE, respectively. The five groups are as follows: for GC ratio, 0.2-0.3, 0.3-0.35, 0.35-0.4, 0.4-0.45, and >0.45; for nucleosome enrichment, 1-8, 9-16, 17-24, 25-39, and >39 counts (*19*); for H3K9me2, <0.5, 0.5-1.25, 1.25-2, 2-3, and >3 $\log_2$ (IP/input) (*20*); for distance to TE edge, <50 bp, 50-100 bp, 100-150 bp, 150-200 bp, and 200-250 bp.

Correlation with histone modifications. Spearman correlation coefficients between TE methylation changes and histone modifications were calculated using 50-bp windows. Data for nucleosomes were derived from (*19*); for H3K9me2 from (*20*); for H3K27me3 from (*21*), and for all other histone modifications from (*10*).

Identification of DMRs and overlaps with imprinted loci. Fractional CG methylation in 50-bp windows across the genome was compared between *dme* endosperm and wild-type endosperm and also between the sperm cell and vegetative cell. Windows with a fractional CG methylation difference of at least 0.3 in the endosperm comparison (Fisher's exact test p-value < 0.001) and at least 0.5 in the vegetative cell comparison (Fisher's exact test p-value < 10^{-10}) were merged to generate larger differentially methylated regions (DMRs) if they occurred within 300 bp. DMRs were retained for further analysis if the fractional CG methylation across the whole DMR was 0.3 greater in *dme* endosperm than in wild-type endosperm or 0.5 greater in the sperm cell than in the vegetative cell (Fisher's exact test p-value < 10^{-10} in both cases), and if the DMR was at least 100 bp. We thus generated 9,816 endosperm DMRs and 9,932 pollen DMRs.

The list of *A. thaliana* imprinted genes was obtained by combining the 114 maternally-expressed genes and 9 paternally-expressed genes from (*4*), 39 maternally-expressed genes and 27 paternally-expressed genes from (*22*) and 165 maternally-expressed genes and 43 paternally-expressed genes from (*23*). DMR distribution with respect to imprinted genes is shown in fig. S7.

Artificial microRNA transgene construction and analysis. We used the *AGL61* promoter to express an artificial microRNA directed against the *GFP* transcript specifically in the central cell (*24*). The *AGL61* promoter was PCR amplified from Col-0 genomic DNA using the primers AGL61F-salI (5'-TGATTACGCCGTCGACAGATGATTTTAGAGTCTCCCGC-3') and AGL61R-asc1 (5'- CTCACCATGGCGCGCCTGTAACATACATTTGTAATTACTCG-3'). The *AGL61* promoter was then cloned into the *LAT52p-amiRNA=GFP* plasmid described in (*7*), replacing the *LAT52* promoter at the SalI and AscI sites to create the *AGL61p-amiRNA=GFP* transgene. As a negative control, the *amiRNA-GFP* fragment was removed by EcoRI digestion followed by self-ligation of the remaining plasmid to create the *AGL61p* transgene. As a positive control, we used the *DD45* promoter to express an artificial microRNA directed against the *GFP*

transcript specifically in the egg cell (*25*). The *DD45* promoter was amplified from Col-0 genomic DNA using primers DD45F-SalI (5'-GACTGTCGACTAAATGTTCCTCGCTGACGT-3') and DD45R-AscI (5'-CTAGGCGCGCCTGTGTTAGAAGCCATTATTC-3'). The DD45 promoter was inserted into the *LAT52p-amiRNA=GFP* plasmid, replacing the *LAT52* promoter at the SalI and AscI sites to create the *DD45p-amiRNA=GFP* transgene.

Transgenic lines and microscopy analysis. Using Agrobacterium-mediated floral dip transformation (*26*), the *AGL61p-amiRNA=GFP*, *AGL61p,* or *DD45p-amiRNA=GFP* transgenes were transformed into a *DD45p-GFP* homozygous reporter line that expresses GPF specifically in the egg cell (*25*). Transgenic seeds were selected on plates with hygromycin antibiotic. PCR procedures were used to detect the presence of the *AGL61p-amiRNA=GFP*, *AGL61p,* or *DD45p-amiRNA=GFP* transgenes as well as the *DD45p-GFP* reporter transgene in hygromycin-resistant T1 seedlings. We monitored the intensity of GFP fluorescence in T1 plants. Anthers were removed from stage 12 to 13 flower buds to prevent fertilization (*27*). Carpels were dissected 48 hours later and GFP fluorescence in intact unfertilized ovules was observed as described previously (*28*). GFP intensity was visually scored and grouped into two categories: strong GFP fluorescence versus faint or no GFP fluorescence. Resistance to hygromycin antibiotic was used to genotype plants for the *AGL61p-amiRNA=GFP* transgene.

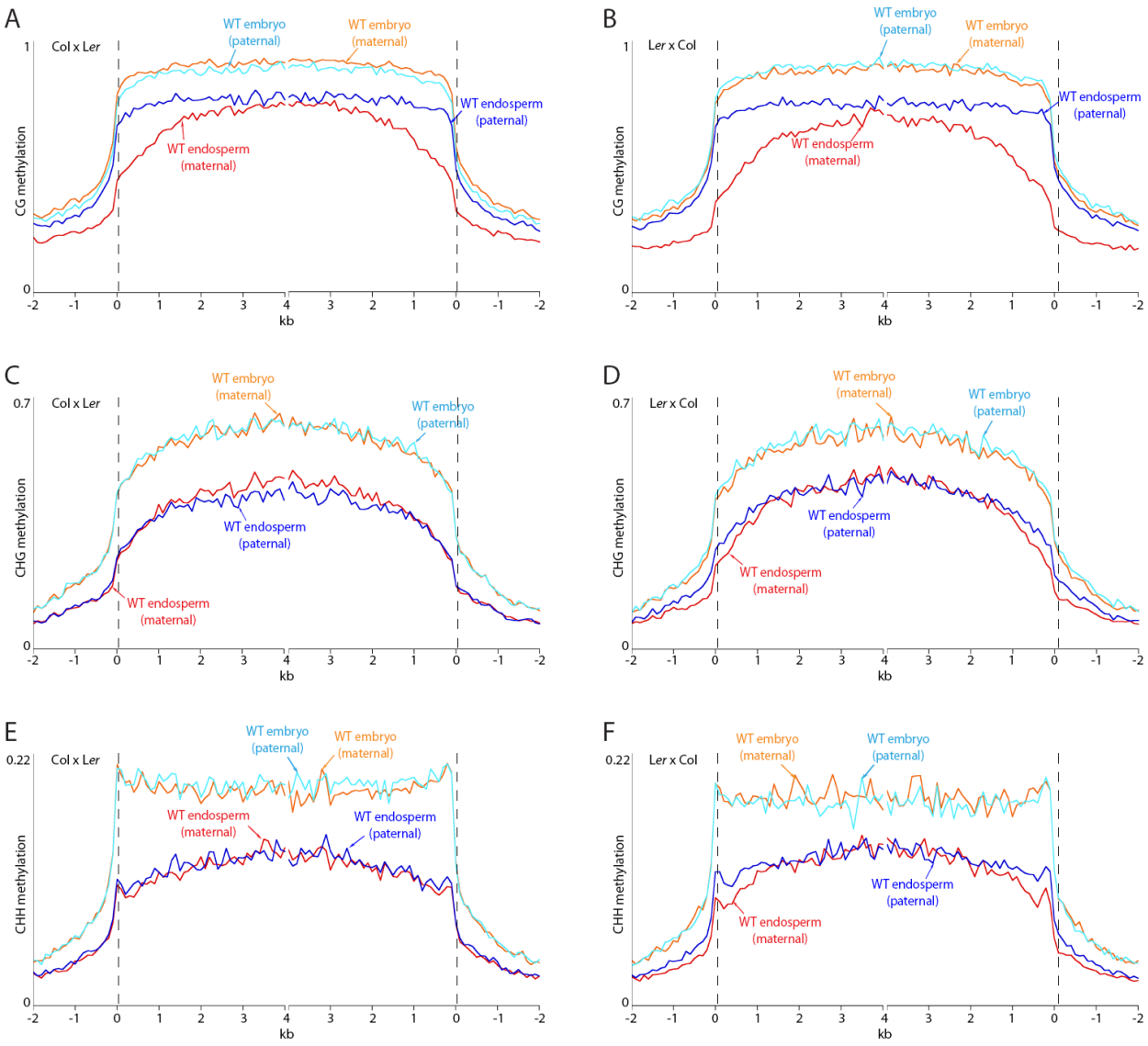

Fig. S1. DNA methylation of transposons in *A. thaliana* seed. (**A-F**) *A. thaliana* transposons were aligned at the 5' end (left panel) or the 3' end (right panel) and average methylation levels for each 100-bp interval are plotted for endosperm and embryo derived from Col x L*er* F1 seeds (**A, C, E**) and L*er* x Col F1 seeds (**B, D, F**). The dashed line at zero represents the point of alignment. CG methylation is shown in (**A-B**), CHG in (**C-D**), CHH in (**E-F**).

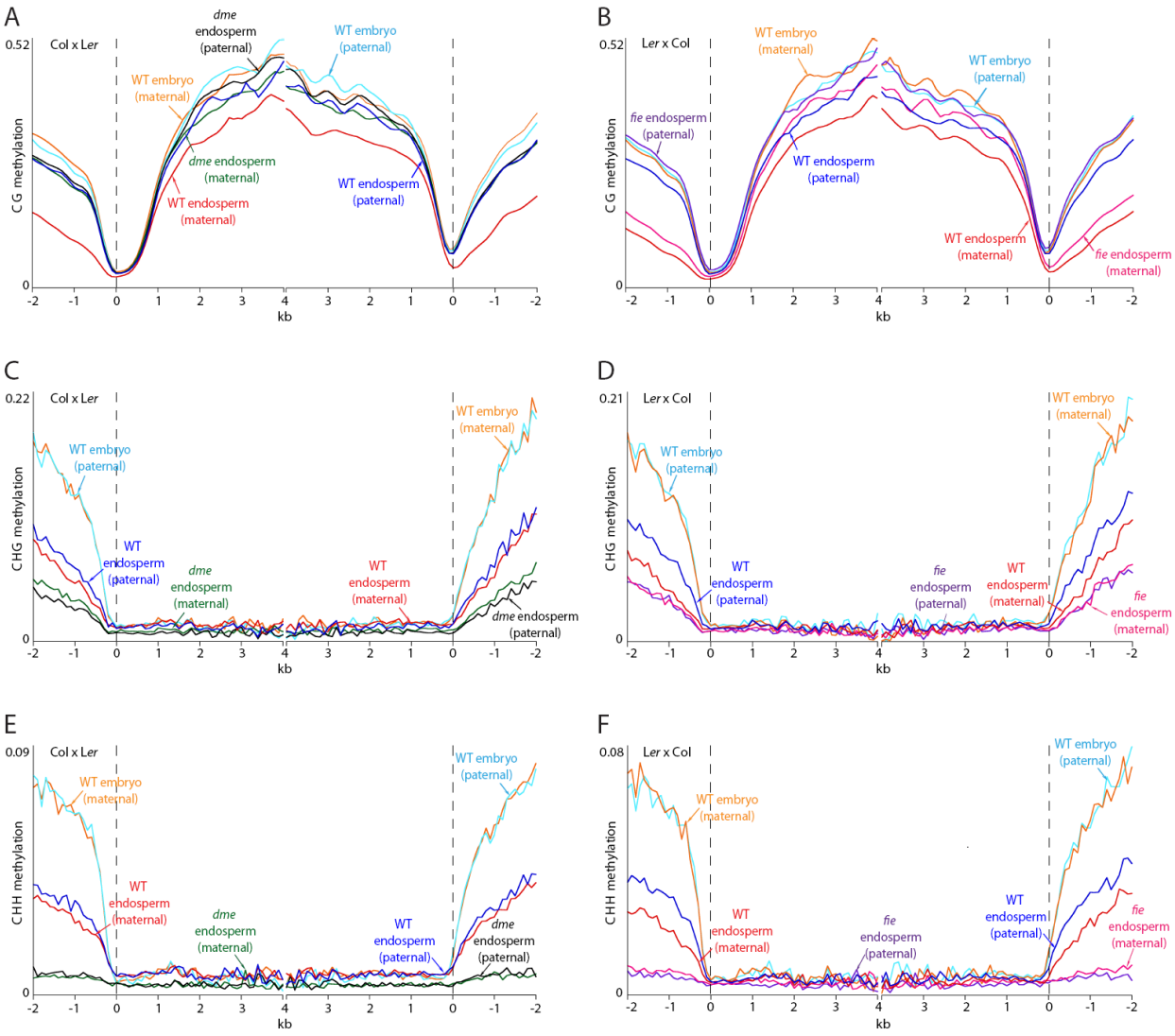

Fig. S2. DNA methylation of genes in the seed. (**A-F**) *A. thaliana* genes were aligned at the 5' end (left panel) or the 3' end (right panel) and average methylation levels for each 100-bp interval are plotted for endosperm derived from Col x L*er* and *dme-2* (Col) x L*er* F1 seeds, and embryo derived from Col x L*er* seeds (**A, C, E**), and for endosperm derived from L*er* x Col and *fie-1* (L*er*) x Col F1 seeds, and embryo derived from L*er* x Col seeds (**B, D, F**). The dashed line at zero represents the point of alignment. CG methylation is shown in (**A-B**), CHG in (**C-D**), CHH in (**E-F**).

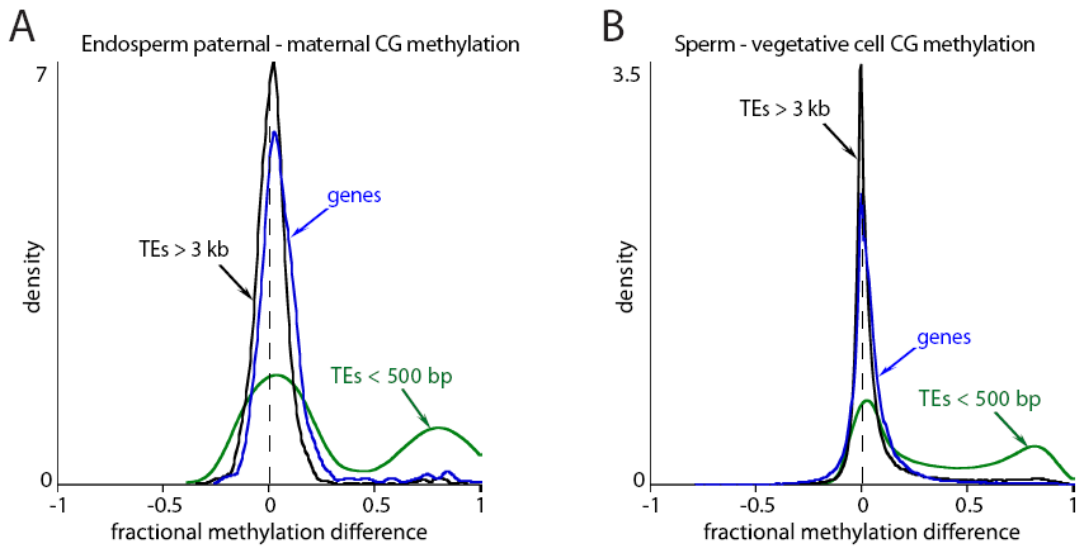

Fig. S3. Maternal demethylation in genes and transposons (TEs). (**A**-**B**) Kernel density plots trace the frequency distribution of the differences between *A. thaliana* paternal and maternal endosperm CG methylation (**A**), and sperm and vegetative cell CG methylation (**B**).

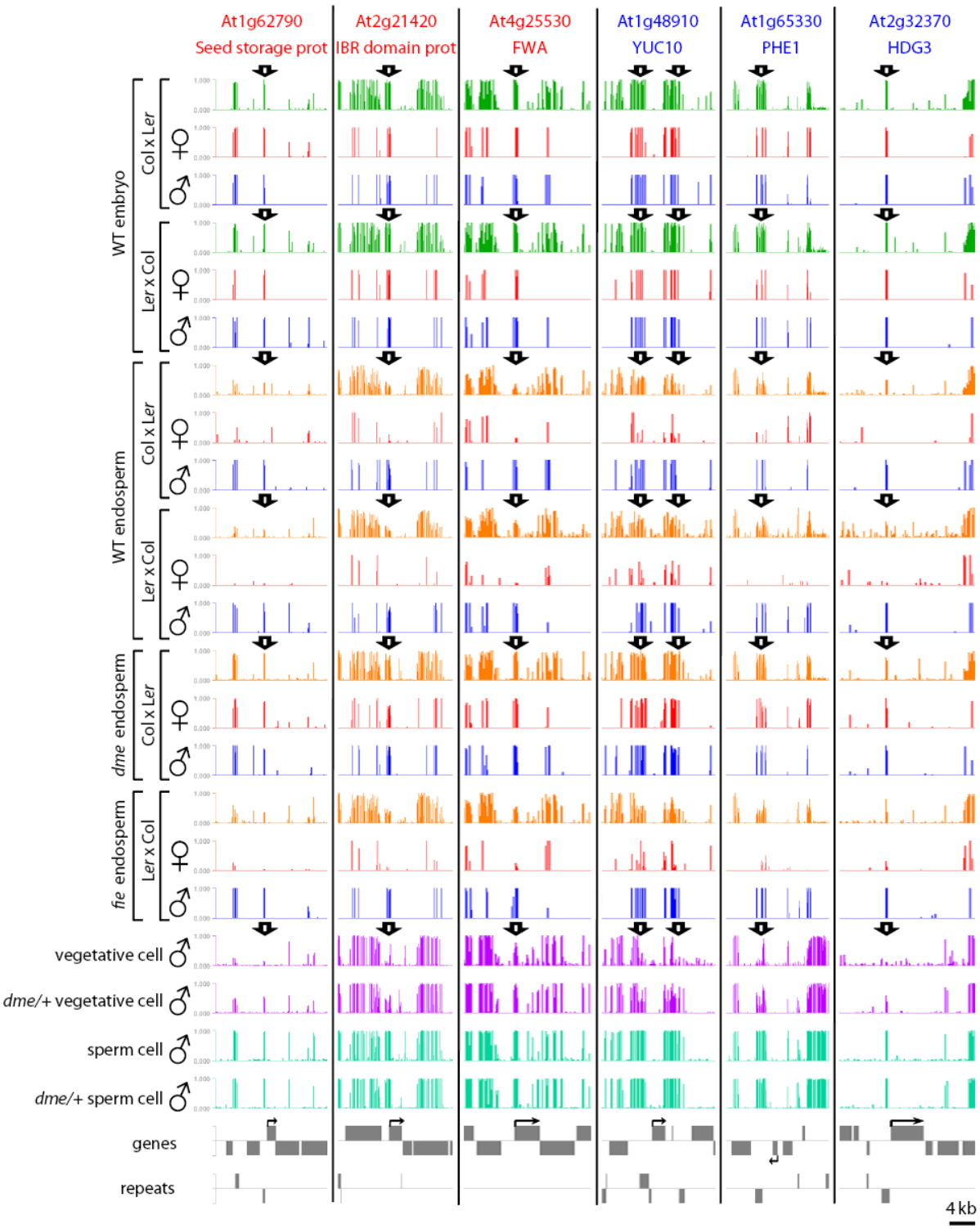

Fig. S4. CG methylation near *A. thaliana* imprinted genes. Snapshots of CG methylation in indicated tissues near maternally expressed (red) and paternally expressed (blue) *A. thaliana* imprinted genes. Green bars represent embryo methylation, orange bars represent endosperm methylation, and red and blue bars represent methylation of the maternal and paternal genomes, respectively. Arrows point out methylation changes in endosperm and vegetative cell.

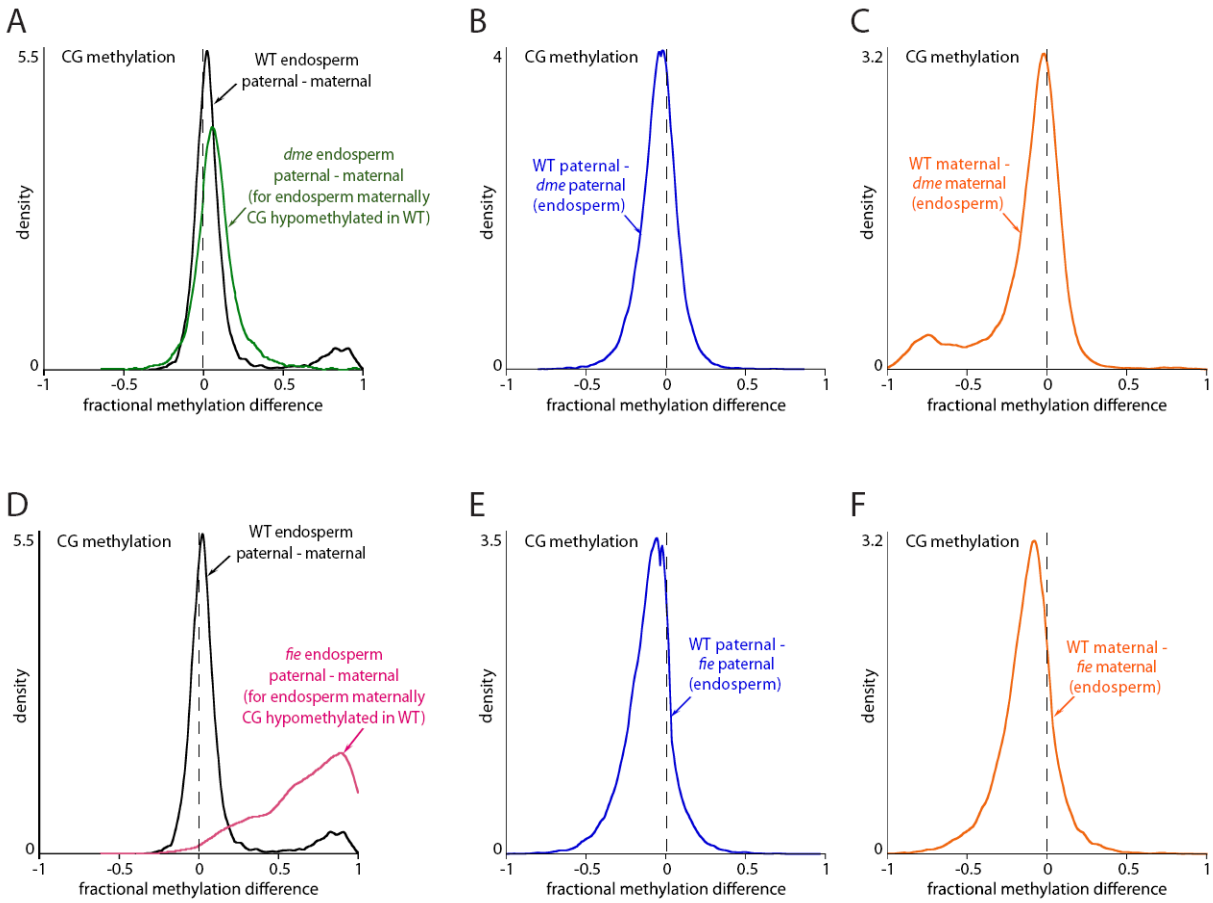

Fig. S5. DNA methylation in *dme* and *fie* endosperm. (**A-F**) Kernel density plots trace the frequency distribution of the *A. thaliana* CG methylation differences between the indicated endosperm genomes.

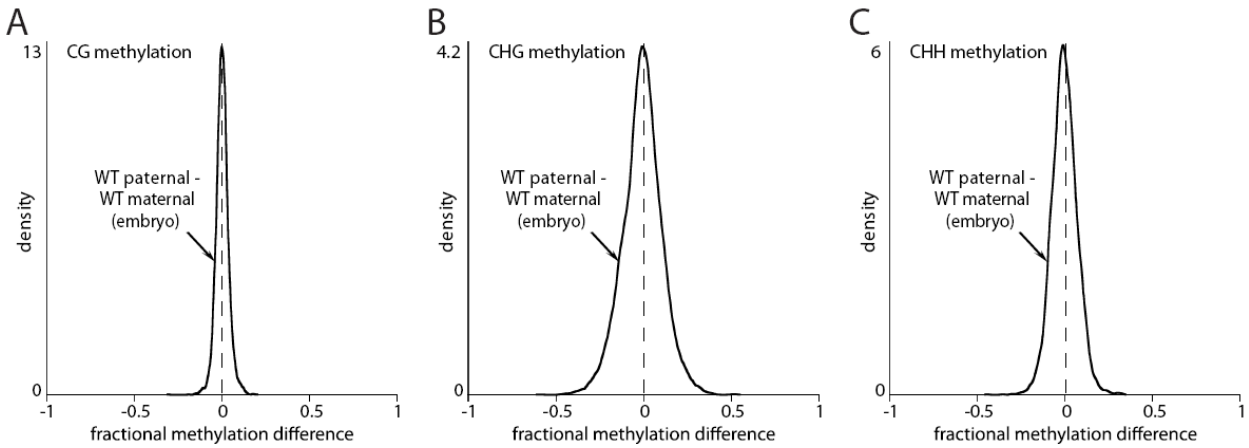

Fig. S6. DNA methylation in *A. thaliana* embryo. (**A-C**) Kernel density plots trace the frequency distribution of the differences between paternal and maternal embryo methylation in *A. thaliana*.

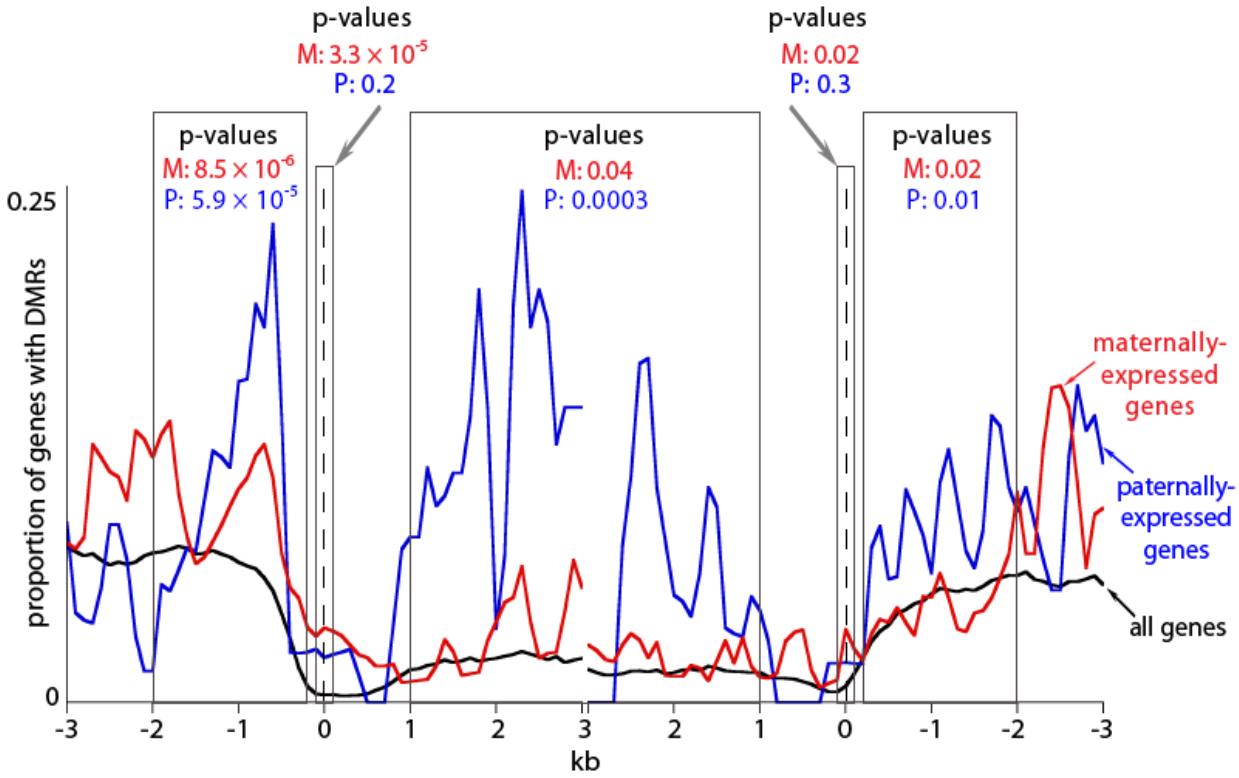

Fig. S7. Endosperm DNA demethylation near imprinted genes. Distribution of significantly differentially methylated regions between wild-type and *dme* mutant endosperm (DMRs) near *A. thaliana* genes. Genes were aligned at the 5' end (left dashed line) or the 3' end (right dashed line) and the proportion of genes with DMRs in each 100-bp interval is plotted. DMR distribution is shown with respect to maternally expressed imprinted genes (red trace), paternally expressed imprinted genes (blue trace) and all genes (black trace). Significance of DMR enrichment with respect to all genes (Fisher's exact test) for particular genic regions is shown in gray boxes.

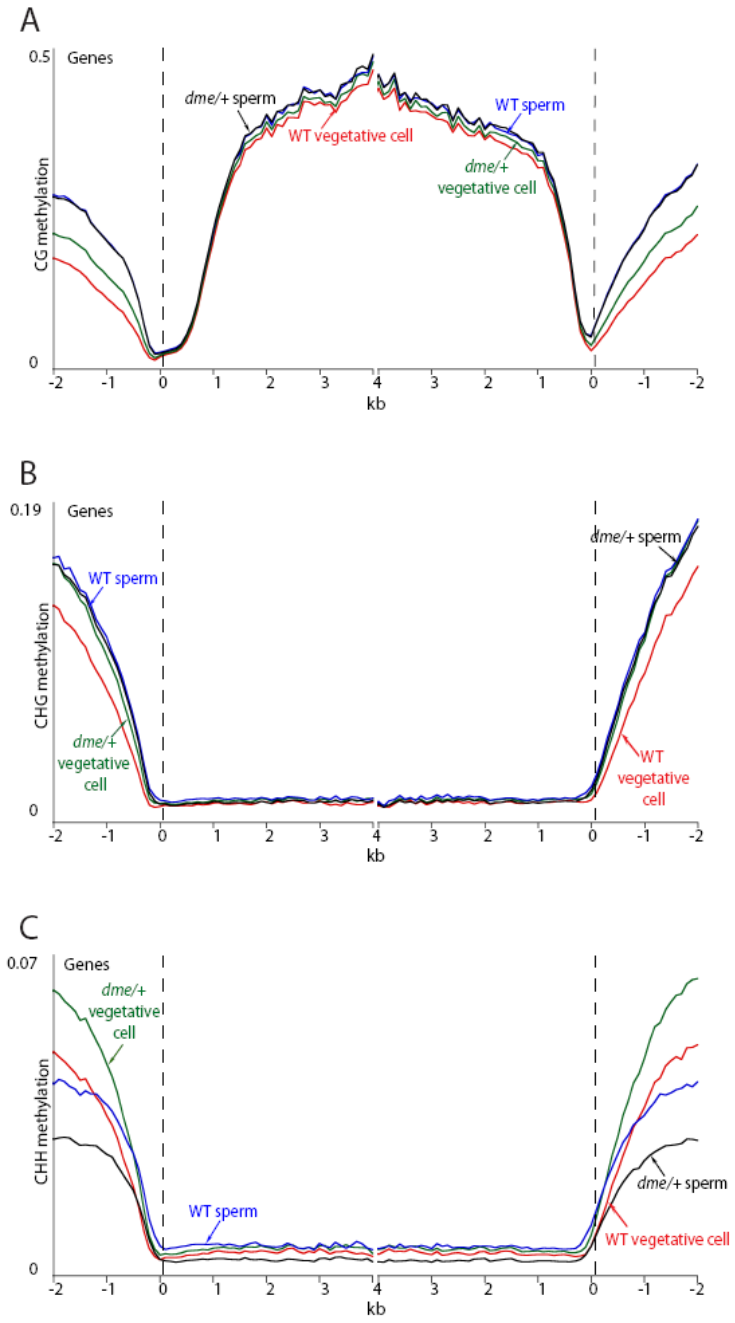

Fig. S8. Pollen DNA methylation in genes for wild-type and *dme-2*/+. (**A-C**) *A. thaliana* genes were aligned at the 5' end (left panel) or the 3' end (right panel) and average methylation levels for each 100-bp interval are plotted for vegetative and sperm cell genomes derived from wild-type and *dme-2*/+ pollen. The dashed line at zero represents the point of alignment. CG methylation is shown in (**A**), CHG in (**B**), CHH in (**C**). Note that WT vegetative cell CHG methylation is lower than sperm CHG methylation near genes (**B**) because small TEs that are preferentially demethylated by DME in vegetative cell nuclei cluster near genes (Fig. 3C). Likewise, CHH methylation in vegetative cells is lower than in sperm immediately adjacent to genes, but becomes higher than in sperm further from genes (**C**).

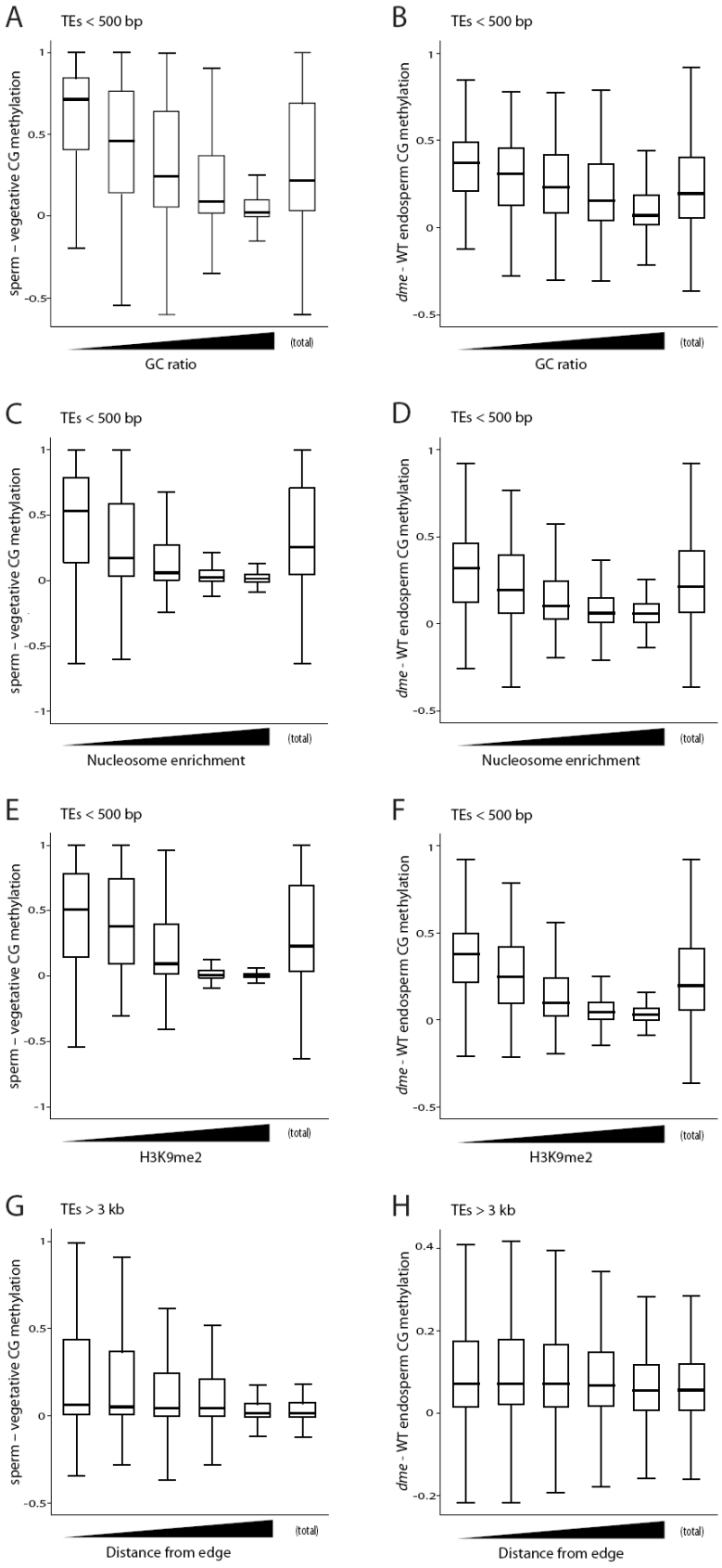

Fig. S9. DNA demethylation in transposons in relation to genomic features. (**A-H**) Box plots showing absolute fractional demethylation of 50-bp windows within transposons. Each box encloses the middle 50% of the distribution, with the horizontal line marking the median, and vertical lines marking the minimum and maximum values that fall within 1.5 times the height of the box. Differences between the first and the fifth categories from the left are significant for all panels ($p<0.001$, Kolmogorov-Smirnov test).

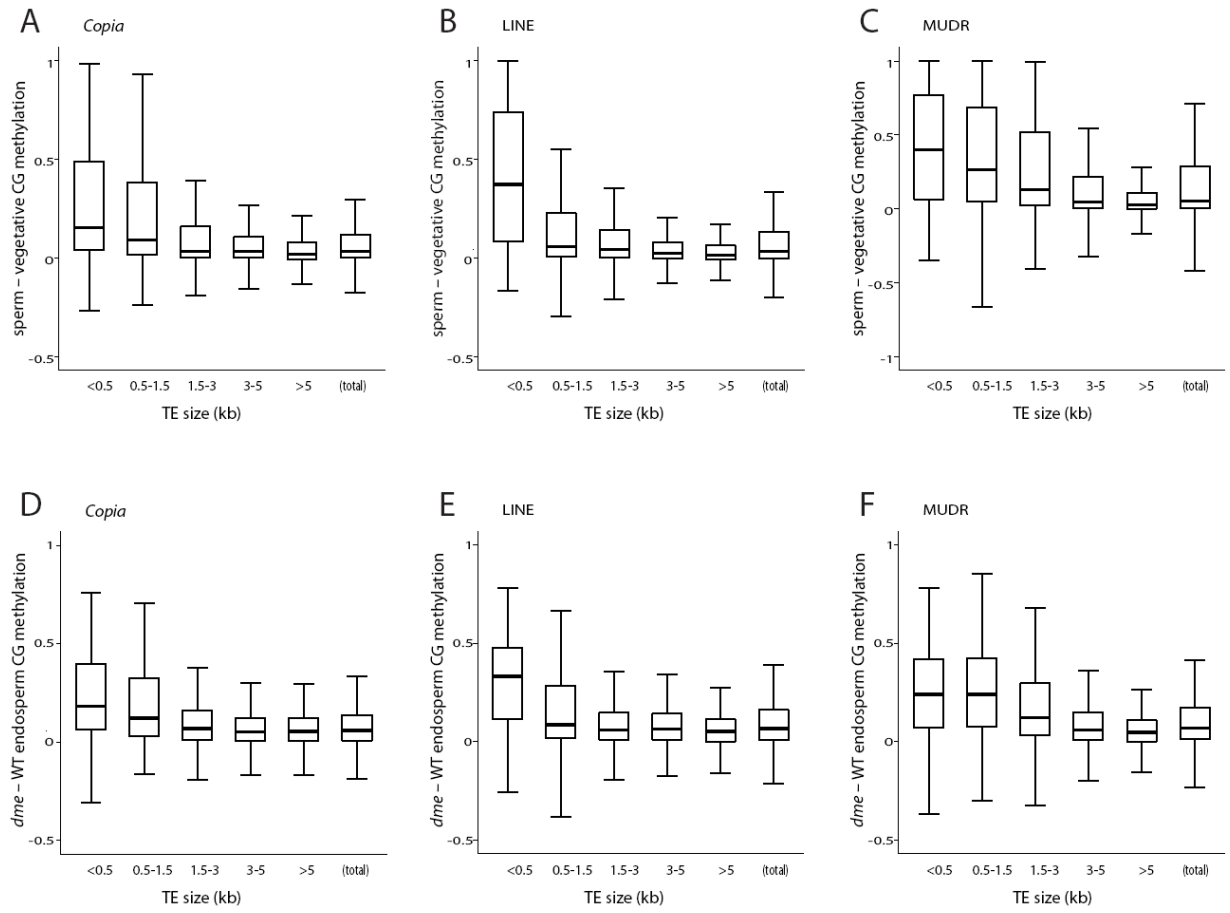

Fig. S10. Small TEs are preferentially demethylated regardless of type. (**A-F**) Box plots showing absolute fractional demethylation of 50-bp windows within three families of transposons: *Copia* (LTR retrotransposon), LINE (non-LTR retrotransposon) and MuDR (DNA transposon). Each box encloses the middle 50% of the distribution, with the horizontal line marking the median. The lines extending from each box mark the minimum and maximum values that fall within 1.5 times the height of the box. Sperm-vegetative differences are shown in (**A-C**) and *dme*-WT endosperm differences in (**D-F**). Differences between the first (<0.5 kb) and the fifth (>5 kb) categories are significant for all panels ($p<0.001$, Kolmogorov-Smirnov test).

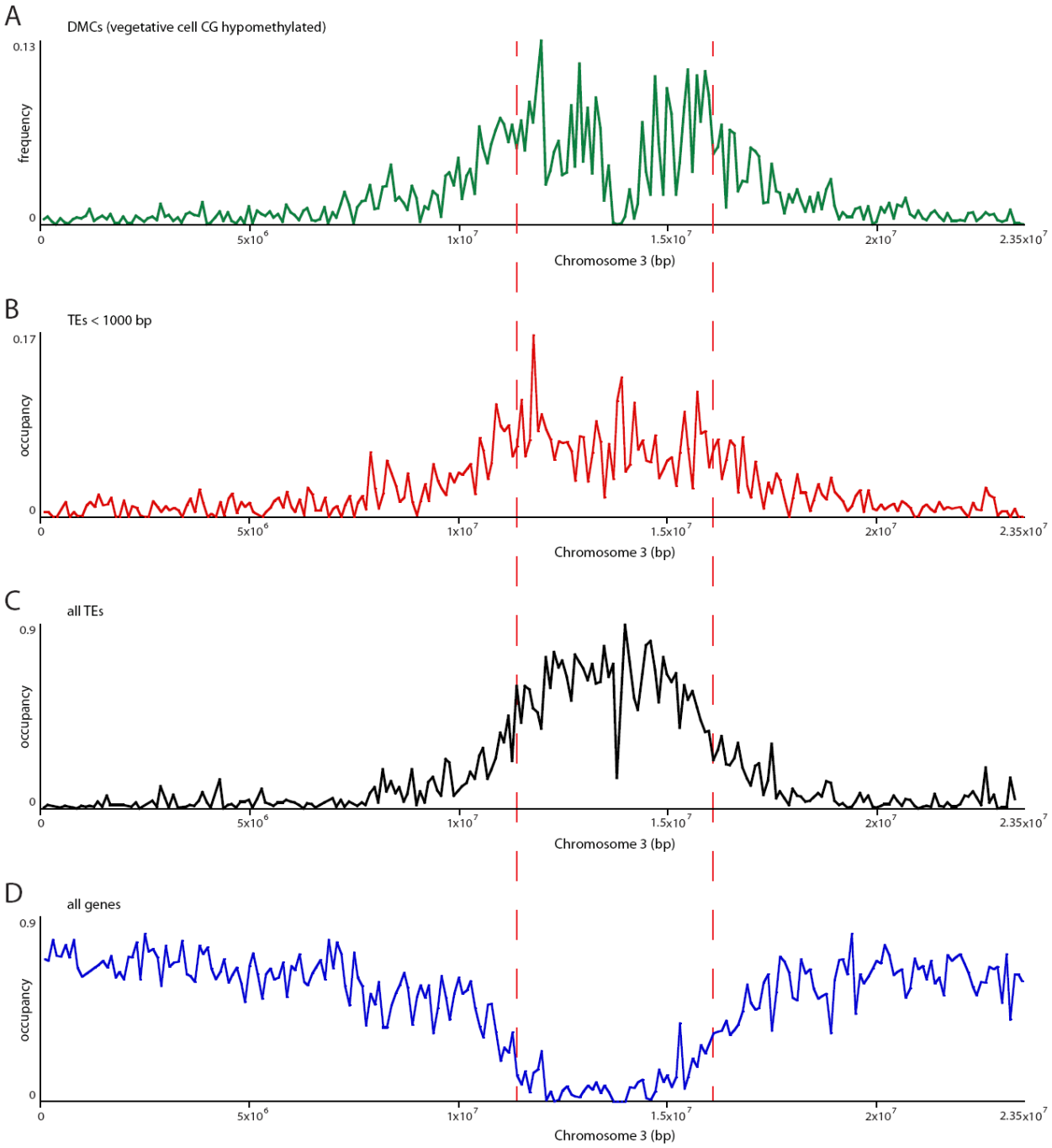

Fig. S11. Distribution of CG sites demethylated in vegetative nuclei. (**A-D**) Distribution across *A. thaliana* chromosome 3 of significantly differentially methylated cytosines (DMCs; p-value < 0.0001, Fisher's exact test) in the CG context that are less methylated in wild-type vegetative cells than in sperm (**A**), transposable elements smaller than 1 kb (**B**), all transposable elements (**C**), and genes (**D**). The dashed lines roughly mark the boundaries of pericentric heterochromatin.

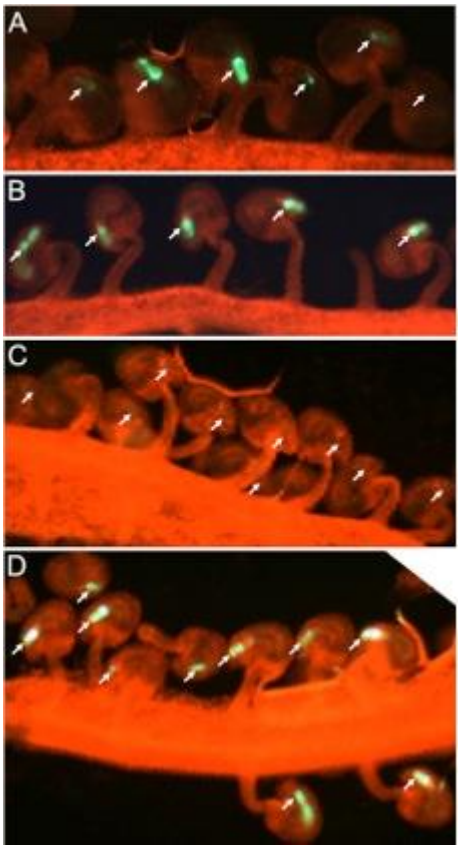

Fig. S12. An anti-GFP microRNA expressed in the central cell correlates with reduced GFP in the egg. To test whether sRNAs can travel from the central cell to the egg, we expressed a microRNA in the central cell that targets cleavage of *GFP* RNA expressed from a transgene in the egg. **(A)** Egg cell GFP expression in a primary transgenic line (table S5, line 2) hemizygous for a transgene expressing an anti-GFP microRNA in the central cell. **(B)** Egg cell GFP expression in a control primary transgenic line (table S5, line 7) lacking the microRNA. **(C)** Egg cell GFP expression that is nearly completed silenced in a plant that is the progeny of the line shown in (**A**) (table S5, line 2e). **(D)** Egg cell GFP expression that is not silenced in a plant that is the progeny of the line shown in (**A**) (table S5, line 2a). All lines are homozygous for the transgene that expresses *GFP* in the egg. Arrows point to egg cells. The promoter used for central cell-specific expression, *AGL61*, does not display detectable activity in the egg cell, or during early female gametophyte development prior to cellularization, when used by others (*24*). However, we cannot rule out the possibility of low-level expression of the anti-GFP microRNA prior to cellularization in the female gametophyte or in the egg cell in the independent transgenic lines we generated (table S5). Further experiments are required to determine whether 24-nt sRNA molecules that mediate DNA methylation are also able to move.

Sample	Median Coverage	Methylation (%) Nuclear CG	Nuclear CHG	Nuclear CHH	Chloroplast CHH	M/P ratio
Col x L*er* embryo	5	29.2	11.8	4.6	0.1	0.96
L*er* x Col embryo	11	29.6	12.1	5.1	0.1	0.93
Col x L*er* endosperm	20	23.7	8.7	3.4	0.4	1.99
L*er* x Col endosperm	29	22.6	8.6	3.0	0.1	1.95
dme-2 x L*er* endosperm	22	27.2	4.7	0.7	0.2	2.09
Col x *fie-1* endosperm	20	26.7	5.6	0.8	0.3	2.06
WT vegetative cell	33	26.9	13.0	4.0	0.3	NA
WT sperm cell	37	31.2	12.7	2.1	0.6	NA
dme-2/+ vegetative cell	45	28.7	14.1	4.7	0.3	NA
dme-2/+ sperm cell	40	31.0	12.4	1.5	0.3	NA

Table S1. Median coverage per cytosine and mean DNA methylation for the indicated samples. Chloroplast CHH methylation is a measure of cytosine non-conversion and other errors. M/P = maternal/paternal; the expected ratio is 1 for embryo and 2 for endosperm. NA = not applicable.

Tissue	Total number	Total bp covered	Minimum length (bp)	Maximum length (bp)	Average length (bp)	% overlap
endosperm	9,816	4,433,250	100	7,750	452	45.5
pollen	9,932	4,068,000	100	6,400	410	49.6

Table S2. Endosperm and pollen DMRs. Continuous differentially methylated regions (DMRs) for endosperm (using the difference between *dme* and WT endosperm) and pollen (using the difference between sperm and vegetative cell). % overlap for endosperm indicates percentage of sequence that overlaps with pollen DMRs, and for pollen indicates percentage of sequence that overlaps with endosperm DMRs.

Endosperm TE size (bp)	% of all demethylated loci	O/E for all loci	p-value for all loci	% of demethylated TE loci	O/E for TE loci	p-value for TE loci
< 500	11.7	3.34	3.4×10^{-43}	29.4	4.14	1.7×10^{-61}
< 1000	19.5	2.95	1.5×10^{-62}	49.1	3.65	2.6×10^{-100}
> 1000	20.2	0.48	9.5×10^{-80}	50.9	0.59	2.6×10^{-100}
> 3000	8.2	0.25	2.2×10^{-118}	20.5	0.31	1.2×10^{-118}

Vegetative cell TE size (bp)	% of all demethylated loci	O/E for all loci	p-value for all loci	% of demethylated TE loci	O/E for TE loci	p-value for TE loci
< 500	8.6	2.67	$< 10^{-299}$	15.8	2.41	$< 10^{-299}$
< 1000	19.4	2.73	$< 10^{-299}$	35.6	2.47	$< 10^{-299}$
> 1000	35.1	0.83	$< 10^{-299}$	64.4	0.75	$< 10^{-299}$
> 3000	14.5	0.46	$< 10^{-299}$	26.6	0.42	$< 10^{-299}$

Table S3. Small TEs are preferentially demethylated. Statistics for fractions of 50-bp windows demethylated in the maternal endosperm genome (top) or in the vegetative cell genome (bottom), as defined in the Materials and Methods for Fig. 1-2, that correspond to transposable elements of various lengths as a fraction of either all loci or of TE loci that are demethylated in the indicated tissue. O/E = observed/expected ratio. Probability values were calculated using Fisher's exact test. Please note that TE annotation is not comprehensive, so the reported TE fractions of total loci are likely underestimates of the actual TE fraction of total loci.

TE	Endosperm maternal/paternal transcript ratio	p-value	Sperm-vegetative cell DMR
AT4TE04415	256	1.60895E-15	Yes
AT4TE08130	69	2.70462E-06	Yes
AT2TE41175	57.33	2.97766E-06	Yes
AT4TE17660	52.36	3.09028E-13	Yes
AT2TE24245	32	0.009	Yes
AT3TE54360	28	0.02	Yes
AT2TE13520	19.33	0.013	Yes
AT3TE63935	18	0.001	Yes
AT5TE44975	15.33	0.028	Yes
AT2TE11110	15	0.015	Yes
AT3TE63215	14.57	0.003	Yes

Table S4. DME-dependent maternally expressed endosperm TEs. TEs specifically expressed from the maternal endosperm genome (Fisher's exact test p-value) that overlap a DME-mediated DMR (table S2) and that are not expressed in *dme* mutant endosperm. All TEs also overlap a sperm-vegetative cell DMR (table S2).

Line	Transgene	No or faint GFP	Strong GFP	N	% GFP	χ^2 (1:1)	P
1	*AGL61p-amiRNA=GFP*	118	102	220	46	1.16	> 0.28
2		106	96	202	48	0.50	> 0.48
3		100	81	181	45	1.99	> 0.16
4		104	112	216	52	0.30	> 0.59
5		105	107	212	50	0.02	> 0.89
6	*AGL61p*	14	199	213	93	-	-
7		16	202	218	93	-	-
8		7	210	217	97	-	-
9		14	201	215	93	-	-
10		16	216	232	93	-	-
11		22	171	193	89	-	-
12		21	205	226	91	-	-
13		15	207	222	93	-	-
14	*DD45p-amiRNA=GFP*	65	50	115	44	2	> 0.16
15		84	130	214	60	10	> 0.002
16		97	105	202	52	0.3	> 0.57
2a	*Line 2, backcrossed & selfed*	30	148	178	83	78	> 0.0001
2b		33	26	59	44	0.83	> 0.36
2c		36	31	67	46	0.37	> 0.54
2d		112	15	127	12	74	> 0.0001
2e		79	7	86	8	60	> 0.0001

Table S5. The indicated transgenes were introduced into lines homozygous for the *DD45p-GFP* reporter gene that expresses *GFP* in the egg cell (*25*). Lines 1-16 represent independent transgenic events. The *AGL61p-amiRNA=GFP* silencer transgene specifically expresses in the central cell (*24*) an artificial microRNA that targets *GFP* RNA. The *AGL61p* transgene is a negative control. The *DD45p-amiRNA=GFP* transgene is a positive control that specifically expresses in the egg cell (*25*) the artificial microRNA that targets GFP RNA. After meiosis, a single hemizygous transgene in the primary T1 line is inherited by 50% of the female gametophytes. If the transgene silences the *DD45p-GFP* reporter, we expect to detect 50% of the egg cells with strong GFP fluorescence and 50% of the egg cells with faint or no GFP fluorescence. We observed this result in lines 1-5 that are hemizygous for the silencer transgene. The same result was observed in the positive control lines 14-16, but not in the negative control transgenic lines 6-13. We analyzed the segregation of the silencer transgene in subsequent generations. Line 2 was backcrossed to a plant homozygous for the *DD45p-GFP* reporter gene. A hemizygous plant from the backcross was self-pollinated and GFP fluorescence in egg cells from progeny (lines 2a-2e) was analyzed. In lines 2d and 2e, most egg cells did not display GFP fluorescence. In lines 2b and 2c, approximately 50% of ovules displayed egg cells with GFP fluorescence. In line 2a, nearly all egg cells displayed GFP fluorescence. N, number of egg cells examined. % GFP, percentage of egg cells with strong GFP fluorescence. χ^2, calculated for a 1:1 segregation of egg cells with no or faint GFP fluorescence versus strong GFP fluorescence. P, probability that the deviation from the expected 1:1 segregation is due to chance.

References and Notes

1. J. A. Law, S. E. Jacobsen, Establishing, maintaining and modifying DNA methylation patterns in plants and animals. *Nat. Rev. Genet.* **11**, 204 (2010).

2. M. J. Bauer, R. L. Fischer, Genome demethylation and imprinting in the endosperm. *Curr. Opin. Plant Biol.* **14**, 162 (2011).

3. T.-F. Hsieh *et al*., Genome-wide demethylation of *Arabidopsis* endosperm. *Science* **324**, 1451 (2009).

4. T.-F. Hsieh *et al*., Regulation of imprinted gene expression in *Arabidopsis* endosperm. *Proc. Natl. Acad. Sci. U.S.A.* **108**, 1755 (2011).

5. Materials and methods are available as supporting material on *Science Online*.

6. M. Gehring *et al*., DEMETER DNA glycosylase establishes *MEDEA* Polycomb gene self-imprinting by allele-specific demethylation. *Cell* **124**, 495 (2006).

7. R. K. Slotkin *et al*., Epigenetic reprogramming and small RNA silencing of transposable elements in pollen. *Cell* **136**, 461 (2009).

8. V. K. Schoft *et al*., Function of the DEMETER DNA glycosylase in the *Arabidopsis thaliana* male gametophyte. *Proc. Natl. Acad. Sci. U.S.A.* **108**, 8042 (2011).

9. V. K. Schoft *et al*., Induction of RNA-directed DNA methylation upon decondensation of constitutive heterochromatin. *EMBO Rep.* **10**, 1015 (2009).

10. F. Roudier *et al*., Integrative epigenomic mapping defines four main chromatin states in *Arabidopsis*. *EMBO J.* **30**, 1928 (2011).

11. W. Qian *et al*., A histone acetyltransferase regulates active DNA demethylation in *Arabidopsis*. *Science* **336**, 1445 (2012).

12. M. Pillot *et al*., Embryo and endosperm inherit distinct chromatin and transcriptional states from the female gametes in *Arabidopsis*. *Plant Cell* **22**, 307 (2010).

13. A. Zemach *et al*., Local DNA hypomethylation activates genes in rice endosperm. *Proc. Natl. Acad. Sci. U.S.A.* **107**, 18729 (2010).

14. R. Lister *et al*., Highly integrated single-base resolution maps of the epigenome in *Arabidopsis*. *Cell* **133**, 523 (2008).

15. J. Penterman *et al*., DNA demethylation in the *Arabidopsis* genome. *Proc. Natl. Acad. Sci. U.S.A.* **104**, 6752 (2007).

16. Y. Choi *et al*., DEMETER, a DNA glycosylase domain protein, is required for endosperm gene imprinting and seed viability in *Arabidopsis*. *Cell* **110**, 33 (2002).

17. N. Ohad *et al*., Mutations in *FIE*, a WD Polycomb group gene, allow endosperm development without fertilization. *Plant Cell* **11**, 407 (1999).

18. A. Zemach, I. E. McDaniel, P. Silva, D. Zilberman, Genome-wide evolutionary analysis of eukaryotic DNA methylation. *Science* **328**, 916 (2010).

19. R. K. Chodavarapu *et al*., Relationship between nucleosome positioning and DNA methylation. *Nature* **466**, 388 (2010).

20. Y. V. Bernatavichute, X. Zhang, S. Cokus, M. Pellegrini, S. E. Jacobsen, Genome-wide association of histone H3 lysine nine methylation with CHG DNA methylation in *Arabidopsis thaliana*. *PLoS ONE* **3**, e3156 (2008).

21. S. Y. Kim, J. Lee, L. Eshed-Williams, D. Zilberman, Z. R. Sung, EMF1 and PRC2 cooperate to repress key regulators of *Arabidopsis* development. *PLoS Genet.* **8**, e1002512 (2012).

22. P. Wolff *et al*., High-resolution analysis of parent-of-origin allelic expression in the Arabidopsis endosperm. *PLoS Genet.* **7**, e1002126 (2011).

23. M. Gehring, V. Missirian, S. Henikoff, Genomic analysis of parent-of-origin allelic expression in *Arabidopsis thaliana* seeds. *PLoS ONE* **6**, e23687 (2011).

24. J. G. Steffen, I. H. Kang, M. F. Portereiko, A. Lloyd, G. N. Drews, AGL61 interacts with AGL80 and is required for central cell development in Arabidopsis. *Plant Physiol.* **148**, 259 (2008).

25. J. G. Steffen, I.-H. Kang, J. Macfarlane, G. N. Drews, Identification of genes expressed in the Arabidopsis female gametophyte. *Plant J.* **51**, 281 (2007).

26. K. S. Century *et al*., NDR1, a pathogen-induced component required for *Arabidopsis* disease resistance. *Science* **278**, 1963 (1997).

27. D. R. Smyth, J. L. Bowman, E. M. Meyerowitz, Early flower development in *Arabidopsis*. *Plant Cell* **2**, 755 (1990).

28. R. Yadegari *et al*., Mutations in the FIE and MEA genes that encode interacting Polycomb proteins cause parent-of-origin effects on seed development by distinct mechanisms. *Plant Cell* **12**, 2367 (2000).

Old refs for comparison, included above:
References

1. Y. Choi *et al.*, *Cell* **110**, 33 (2002).
2. N. Ohad *et al.*, *Plant Cell* **11**, 407 (1999).
3. V. K. Schoft *et al.*, *Proc Natl Acad Sci U S A* **108**, 8042 (2011).
4. V. K. Schoft *et al.*, *EMBO Rep* **10**, 1015 (2009).
5. T.-F. Hsieh *et al.*, *Science* **324**, 1451 (2009).
6. T. F. Hsieh *et al.*, *Proc Natl Acad Sci U S A* **108**, 1755 (2011).
7. A. Zemach, I. E. McDaniel, P. Silva, D. Zilberman, *Science* **328**, 916 (2010).
8. R. K. Chodavarapu *et al.*, *Nature* **466**, 388 (2010).
9. Y. V. Bernatavichute, X. Zhang, S. Cokus, M. Pellegrini, S. E. Jacobsen, *PLoS One* **3**, e3156 (2008).
10. S. Y. Kim, J. Lee, L. Eshed-Williams, D. Zilberman, Z. R. Sung, *PLoS Genet* **8**, e1002512 (2012).
11. F. Roudier *et al.*, *EMBO J* **30**, 1928 (2011).
12. P. Wolff *et al.*, *PLoS Genet* **7**, e1002126 (2011).
13. M. Gehring, V. Missirian, S. Henikoff, *PLoS One* **6**, e23687 (2011).
14. J. G. Steffen, I. H. Kang, M. F. Portereiko, A. Lloyd, G. N. Drews, *Plant Physiol* **148**, 259 (2008).
15. R. K. Slotkin *et al.*, *Cell* **136**, 461 (2009).
16. J. G. Steffen, I.-H. Kang, M. Macfarlane, G. N. Drews, *Plant J* **51**, 281 (2007).
17. K. S. Century *et al.*, *Science* **278**, 1963 (1997).

18. D. R. Smyth, J. L. Bowman, E. M. Meyerowitz, *Plant Cell* **2**, 755 (1990).
19. R. Yadegari *et al.*, *Plant Cell* **12**, 2367 (2000).